

# **Extreme Sampling: Flare Gas**

Hans-Peter Visser  
Analytical Solutions and Products (ASaP)  
Distelweg 80m, 1031 HH Amsterdam  
The Netherlands

## **Keywords**

SAMPLE TAKE-OFF, SAMPLING, PROBE, REPRESENTATIVE SAMPLING, FLARE GAS

## **Abstract**

As per November 2015, flares should comply with Subpart Ja 40CFR60 subpart Ja – Total Sulfur / Hydrogen Sulfide (H<sub>2</sub>S) Measurements and 40CFR60.18 – Net Heating Value. Typically the focus is on the analysis itself and not so much on the sample probe and conditioning system. From experience it's known that good measurement is as good as the weakest part of the chain, meaning from sample take-off to the analyser itself.

The most common challenge of flare gas sampling is that nobody knows what is the exact composition at a given time. It is dependent of the operation of the units upstream.

The flaw of most existing probes and sample conditioning systems is that they are designed to specifications which are typical snap-shots of a lab analysis and most often not based on excessive conditions when the measurements are needed most. A special flare gas probe has been developed taking excessive process conditions in consideration.

## Introduction

A gas flare, alternatively known as a flare stack, is a gas combustion device used in industrial plants such as petroleum refineries, chemical plants and natural gas processing plants as well as at oil or gas production sites having oil wells, gas wells and offshore oil and gas rigs.

In industrial plants, flare stacks are primarily used for burning off flammable gas released by pressure relief valves during unplanned, over-pressuring of plant equipment. During plant or partial plant startups and shutdowns, flare stacks are also often used for the planned combustion of gases over relatively short periods.

A great deal of gas flaring at many oil and gas production sites has to do with protection against the dangers of over-pressuring industrial plant equipment.

When industrial plant equipment items are over-pressured, the pressure relief valve is an essential safety device that automatically release gases and sometimes liquids. Those pressure relief valves are required by industrial design codes and standards as well as by law.

The released gases and liquids are routed through large piping systems called *flare headers* to a vertical elevated flare. The released gases are burned as they exit the flare stacks. The size and brightness of the resulting flame depends upon the flammable material's flow rate in joules per hour (or BTU per hour).

Most industrial plant flares have a vapor-liquid separator (also known as a knockout drum) upstream of the flare to remove any large amounts of liquid that may accompany the relieved gases.

Steam is very often injected into the flame to reduce the formation of black smoke. When too much steam is added, a condition known as "over steaming" can occur, resulting in reduced combustion efficiency and higher emissions. To keep the flare system functional, a small amount of gas is continuously burned, a pilot light, so that the system is always ready for its primary purpose as an over-pressure safety system.

Figure 1. illustrates a flow diagram depicting the typical components of an overall industrial flare stack system:

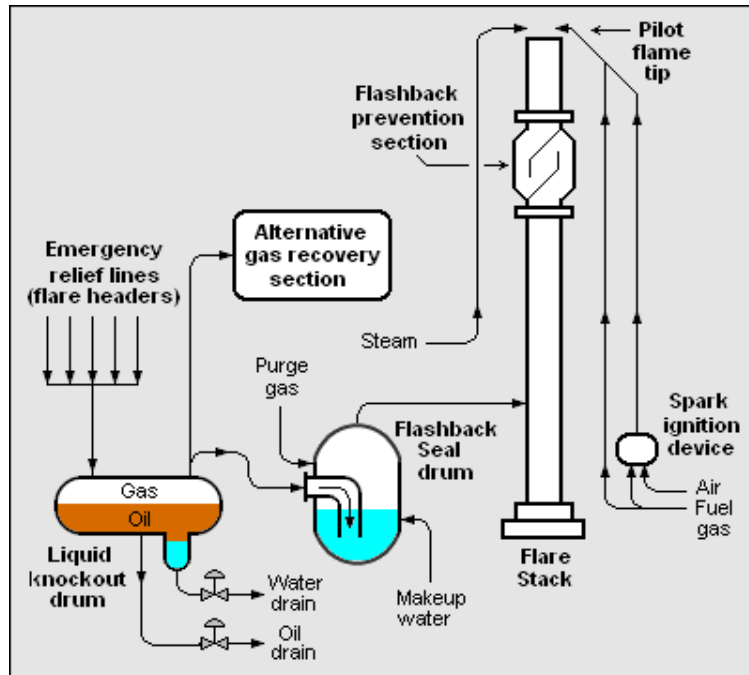


**FIGURE 1. FLOW DIAGRAM FLARE STACK SYSTEM.**

- A knockout drum to remove any oil and/or water from the relieved gases.
- A water seal drum to prevent any flashback of the flame from the top of the flare stack.
- An alternative gas recovery system for use during partial plant startups and/or shutdowns as well as other times when required. The recovered gas is routed into the fuel gas system of the overall industrial plant.
- A steam injection system to provide an external momentum force used for efficient mixing of air with the relieved gas, which promotes smokeless burning.
- A pilot flame (with its ignition system) that burns all the time so that it is available to ignite relieved gases when needed.
- The flare stack, including a flashback prevention section at the upper part of the stack.

### **Sampling challenge**

As per November 2015, flares should comply with Subpart Ja 40CFR60 subpart Ja – Total Sulfur / Hydrogen Sulfide (H<sub>2</sub>S) Measurements and 40CFR60.18 – Net Heating Value. These analyses must have a high availability under all circumstances.

The real challenge of sampling and analyzing flare gas is, no one knows which components and their associated concentrations are present at a specific time. A good indication can be obtained by periodically taking lab samples, but these remain a snap shot in time.

It is even worse when industrial plant equipment items are over-pressured or have any other process upset conditioning, the composition and its concentrations may vary instantaneously, including pressure fluctuations and extreme increase of process volume and its velocity. It is possible to have process stream velocities of 100 m/s to occur, in these process upset conditions.

Consequentially fouling, contamination, particles, etc. will increase most often even more during upset conditions. Especially fouling, contamination cause the sampling challenge, often plugging of small bore tubing such as used in the analyzer sampling systems.

### **Knowing the characteristics of upstream processes**

It is essential for a proper analyzer system design, to know and understand all upstream processes especially their behaviors during upset conditions. By knowing these upset characteristics, adequate anticipation in system design can be taken into account.

Most refineries and gas treating plants which are using a sour (acid) feedstock requiring amine treaters and sulphur recovery units. These units are typically not the “money-makers” of a refinery or gas plant, they are essential for environmental control. Severe changes in feedstock, improper operation, lack of maintenance, lack of process knowledge of these units are most often the root cause of fouling and plugging of analyzer systems.

Classical examples are the presence of heat stable salts (most often ammonia salts) and elementary sulphur. This are typically the species which are the root cause of fouling and plugging.

### **Knowing the exact analytical requirements**

A good analytical specification is an art on its own. Unfortunately the essentials of the analysis is sometimes missing or even worse a specification is a matter of “Copy & Paste” of similar projects including their design errors.

A good specification starts with the reason of the analysis, followed by the purpose of the analysis and finally by the criticality of the analysis. These specifications are the start of a proper analyzer selection and proper system design. Each process is unique, despite the equality on paper or its license. Operation of process units will be affected by environmental conditions, feed stock, local requirements etc.

Examples of reason of analysis are i.e.: legalization, product quality, energy efficiency, environmental, safety, management or process reliability

Examples of purpose of measurement are i.e.: trending, monitoring, control, alarm or trip.

Examples of critically are i.e.: safety, process, environment, quality or none critical.

For this flare gas project the Analytical Narrative Online Process Analyser are given in Table I.

**TABLE I. Analytical Narrative Online process Analyser**

1. REASON AND PURPOSE OF MEASUREMENT							
Reason of measurement	Yes/No		Purpose of measurement	Yes/No		Criticality analyser	Yes/No
client (external/internal)	<input checked="" type="checkbox"/> / <input type="checkbox"/>		Trending	<input checked="" type="checkbox"/> / <input type="checkbox"/>		Safety	<input checked="" type="checkbox"/> / <input type="checkbox"/>
legislation	<input checked="" type="checkbox"/> / <input type="checkbox"/>		monitoring	<input checked="" type="checkbox"/> / <input type="checkbox"/>		Process	<input checked="" type="checkbox"/> / <input type="checkbox"/>
product quality	<input checked="" type="checkbox"/> / <input type="checkbox"/>		control	<input type="checkbox"/> / <input type="checkbox"/>		Environment	<input checked="" type="checkbox"/> / <input type="checkbox"/>
energy efficiency	<input checked="" type="checkbox"/> / <input type="checkbox"/>		alarm	<input checked="" type="checkbox"/> / <input type="checkbox"/>		Quality	<input checked="" type="checkbox"/> / <input type="checkbox"/>
environmental	<input checked="" type="checkbox"/> / <input type="checkbox"/>		trip	<input type="checkbox"/> / <input type="checkbox"/>		Not critical	<input type="checkbox"/> / <input type="checkbox"/>
safety	<input checked="" type="checkbox"/> / <input type="checkbox"/>						
management	<input checked="" type="checkbox"/> / <input type="checkbox"/>					Safety Integrity Level	N/A
process reliability	<input checked="" type="checkbox"/> / <input type="checkbox"/>						
<b>REMARKS:</b>							

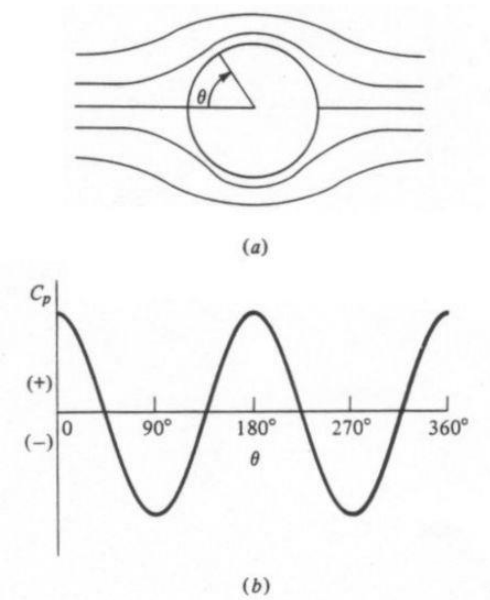
## 1. Multi stage sample take-off probe

Due to the nature of the upstream processes and their characteristic behavior especially during upset conditions, the flare gas probe consists of multiple stages to ensure reliable and high availability of downstream systems and analyzers.

### 1.1 First stage: Probe aerodynamics

The aerodynamics of the probe tip and location of sample entrance in the probe, minimize entrance into the probe of particles, liquid carry-over, droplets, dirt and aerosols. Potential contaminants are drained automatically in case of an eventual liquid carry-over.

In an ideal world, without any friction, the air flowing around a smooth sphere would behave like that shown in Figure 2. In this Figure, the angle  $\theta$  represents the position along the surface of the sphere. The leading edge of the sphere that first encounters the incoming airflow is at  $\theta=0^\circ$  while the trailing edge is at  $\theta=180^\circ$ . A position of  $\theta=90^\circ$  is the top of the sphere,  $\theta=270^\circ$  is the bottom, and  $\theta=360^\circ$  brings us back around to the leading edge. Note that in this ideal situation, the air flowing around the sphere forms a perfectly symmetrical pattern. The streamline pattern around the front face, from  $270^\circ$  up to  $90^\circ$ , is the same as that around the back face, from  $90^\circ$  down to  $270^\circ$ .



(a) Ideal frictionless flow field around a sphere and  
(b) resulting pressure distribution

**FIGURE 2. AIR FLOW PROFILE AROUND SMOOTH SPHERE.**

The lower half of this Figure also displays the pressure distribution around the surface of the sphere, as represented by the non-dimensional pressure coefficient  $C_p$ . Positive (+) values of  $C_p$  indicate high pressure while negative (-) values indicate low pressure. It is the differences between high-

pressure regions and low-pressure regions that create aerodynamic forces on a body, like lift and drag.

However, this ideal flow pattern tells us something very interesting. Notice that the pressure at the front of the sphere, or  $\theta=0^\circ$ , is very high. This high pressure indicates that the incoming air impacting against the front face creates a drag force. Nonetheless, the pressure at the back of the sphere, or  $\theta=180^\circ$ , is also high and identical to that at the front. This high pressure actually creates a thrust, or negative drag, that cancels out the drag on the front of the sphere. In other words, this theoretical situation tells us that there is no drag on a sphere!

Early aerodynamics researchers were quite puzzled by this theoretical result because it contradicted experimental measurements indicating that a sphere does generate drag. The conflict between theory and experiment was one of the great mysteries of the late 19th century that became known as d'Alembert's Paradox, named for famous French mathematician and physicist Jean le Rond d'Alembert (1717-1783) who first discovered the discrepancy.

The reason d'Alembert's ideal theory failed to explain the true aerodynamic behaviour of a sphere is that he ignored the influence of friction in his calculations. The actual flow field around a sphere looks much different than his theory predicts, because friction causes a phenomenon known as flow separation. We can better understand this effect by studying the diagram as shown in Figure 3 of the actual flow around a smooth sphere. Here we see that the flow field around the sphere is no longer symmetrical. Whereas the flow around the ideal sphere continued to follow the surface along the entire rear face, the actual flow no longer does so. When the airflow follows along the surface, we say that the flow is attached. The point at which the flow breaks away from the surface is called the separation point, and the flow downstream of this point is referred to as separated. The region of separated flow is dominated by unsteady, recirculating vortices that create a wake.

- (a) Actual separated flow field around a sphere and
- (b) resulting pressure distribution.

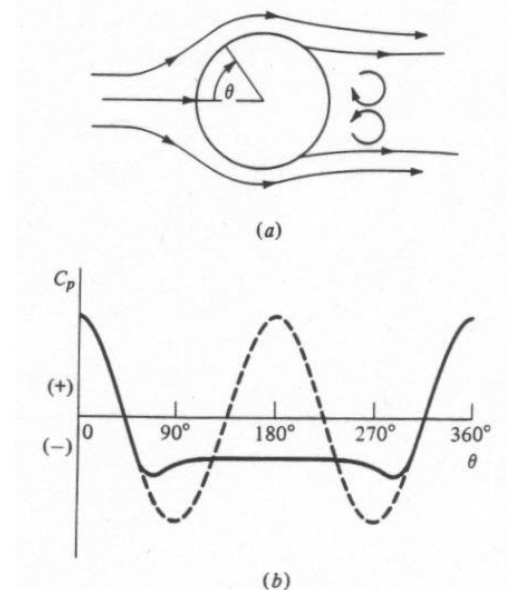


**FIGURE 3. AIR FLOW PROFILE AROUND SMOOTH SPHERE INCLUDING FRICTION TAKING INTO ACCOUNT.**

The cause of this separation can be seen in Figure 3 pressure distribution around the sphere. As the flow moves downstream from the  $\theta=90^\circ$  or  $\theta=270^\circ$  position, it encounters an increasing pressure. Whenever a flow encounters increasing pressure, we say that it experiences an adverse pressure gradient. The change in pressure is called adverse, because it causes the airflow to slow down and lose momentum. As the pressure continues to increase, the flow continues to slow down until it reaches a speed of zero. It is at this point that the air no longer has any forward momentum, so it separates from the surface.

Once the flow separates from the surface, it no longer results in the ideal pressure distribution, shown as the dashed line. Instead, a separated flow creates a region of low pressure in the wake. We see this behaviour over the rear face of the sphere from  $90^\circ < \theta < 270^\circ$ . Here, the actual pressure distribution, shown as the solid line, remains negative, in contrast to the ideal prediction. The pressure on the front face is still high, however, just as it was for the ideal sphere. Since the pressure is now much higher on the front face than it is on the rear face, the net result is a drag force exerted on the sphere. By accounting for the effect of friction, theory and experiment come into agreement and d'Alembert's Paradox is reconciled.

The German physicist Ludwig Prandtl suggested in 1904 that the effects of a thin viscous boundary layer possibly could be the source of substantial drag. Prandtl put forward the idea that, at high velocities and high Reynolds numbers, a no-slip boundary condition causes a strong variation of the flow speeds over a thin layer near the wall of the body. This leads to the generation of vorticity and viscous dissipation of kinetic energy in the boundary layer. The energy dissipation, which is lacking in the inviscid theories, results for bluff bodies in separation of the flow. The low pressure in the wake region causes form drag, and this can be larger than the friction drag due to the viscous shear stress at the wall.

Evidence that Prandtl's scenario occurs for bluff bodies in flows of high Reynolds numbers can be seen in impulsively started flows around a cylinder. Initially the flow resembles potential flow, after which the flow separates near the rear stagnation point. Thereafter, the separation points move upstream, resulting in a low-pressure region of separated flow.

Prandtl made the hypothesis that the viscous effects are important in thin layers – called boundary layers – adjacent to solid boundaries, and that viscosity has no role of importance outside. The boundary-layer thickness becomes smaller when the viscosity reduces. The full problem of viscous flow, described by the non-linear Navier–Stokes equations, is in general not mathematically solvable. However, using his hypothesis (and backed up by experiments) Prandtl was able to derive an approximate model for the flow inside the boundary layer, called *boundary-layer theory*; while the flow outside the boundary layer could be treated using inviscid flow theory. Boundary-layer theory is amenable to the method of matched asymptotic expansions for deriving approximate solutions. In the simplest case of a flat plate parallel to the incoming flow, boundary-layer theory results in (friction) drag, whereas all inviscid flow theories will predict zero drag. Of importance for aeronautics, Prandtl's theory can be applied directly to streamlined bodies like airfoils where, in addition to surface-friction drag, there is also form drag. Form drag is due to the effect of the boundary layer and thin wake on the pressure distribution around the airfoil.



Experiment 3 – flow past a circular cylinder of William J. Devenport involve the study of flow past a circular cylinder in a uniform stream. This is done in a wind tunnel using conventional instrumentation, specifically a Pitot static probe and static pressure ports.

The study and tests describes the pressure distributions on a circular cylinder compared with the theoretical distribution calculated assuming ideal flow. Figure 4 and 5 are illustrating flow patterns of respective flows at subcritical Reynolds number ( $1.86 \times 10^5$ ) and flows at supercritical Reynolds number ( $6.7 \times 10^5$ ).

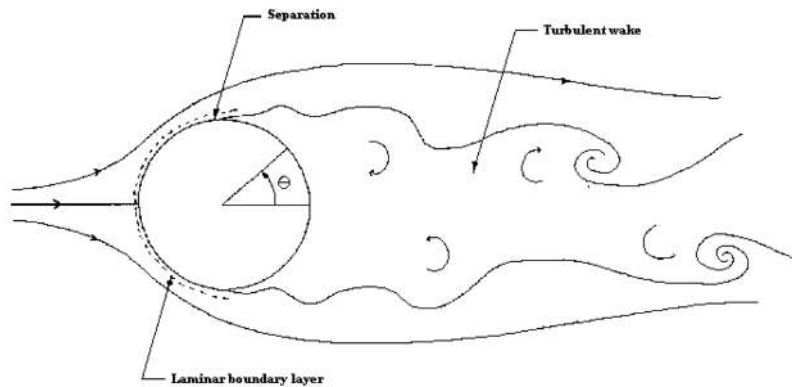


**FIGURE 4. FLOW PATTERN AT SUBCRITICAL REYNOLDS NUMBER.**

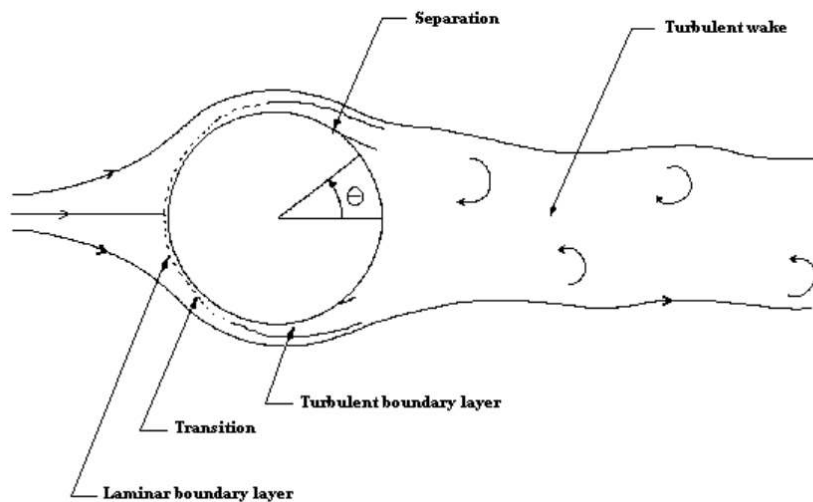


**FIGURE 5. FLOW PATTERN AT SUPERCRITICAL REYNOLDS NUMBER.**

As a result the measured pressure distributions on a circular cylinder are compared with a theoretical distribution calculated assuming ideal flow as given in Figure 6. Angle  $\theta$  is defined as the point of tangency, collateral to the flow.

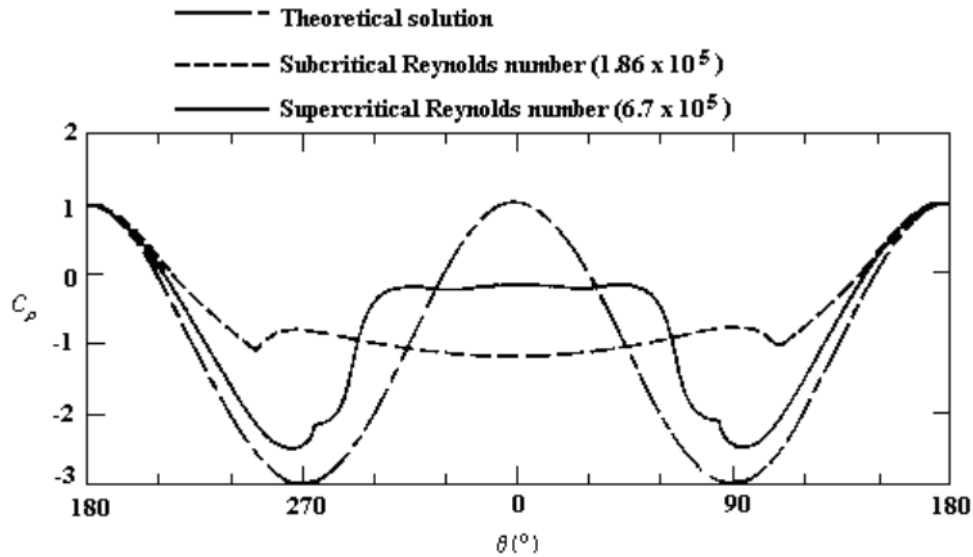


**FIGURE 6. MEASURED PRESSURE DISTRIBUTION ON A CIRCULAR CYLINDER.**

The flare gas probe gas entry point was designed based on this phenomena and validated against Computational Fluid Dynamics (CFD) analysis. The outcome is shown in Figure 7.

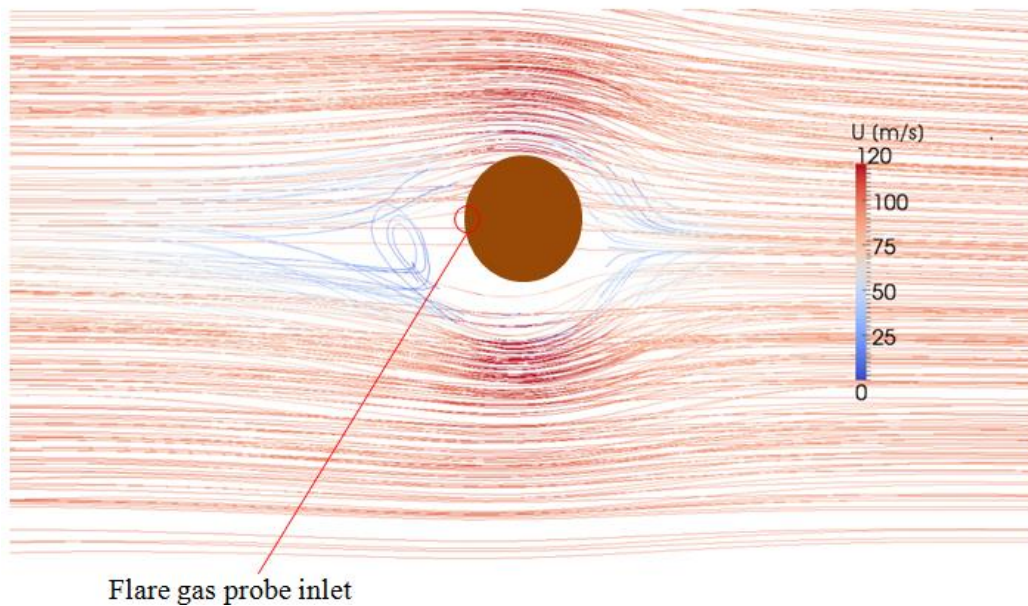


**FIGURE 7. CFD ANALYSIS OF FLARE GAS PROBE.**

## 1.2 Second stage: Inclined Stokes-Law separation

The ability of a probe to ignore solid particles or liquid mist depends on the velocity of the fluid passing through it, relative to velocity of the process stream. When a process velocity is high but the sample gas velocity through the probe is low, the extraction of particles and liquid mist is also low because they tend to fall out by gravity.

Allowing particles or liquid mist to fall back into the process stream simplify the design of the conditioning system downstream of the probe. It actually increases the system reliability and availability.

By gravity, the rate of heavier (most often also larger) particles which fall out is larger than lighter (smaller) particles. George Stokes was the first to explain this phenomenon which was translated to the Stokes Law.

When a particle falls by gravity in a still fluid, it experience a drag force due to the viscosity of the fluid. As a falling particle speeds up, the drag force increase until it becomes equal to the net weight of the particle in the fluid. Once the forces are balanced, the particle fall at a constant speed also known as its terminal velocity or settling velocity for small particles. The settling velocity depends on the particle size.

The settling velocity is always relative to the motion of the fluid. When the fluid is moving upward as the particles descend (Figure 8), particles larger than a certain size are falling faster than the upward flow and continue to fall at a relative slower rate. These particles fall back into the process.

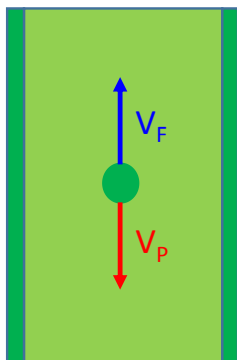


**FIGURE 8. VERTICAL SEPERATION BY STOKES LAW.**

$$D_H = \sqrt{\frac{18 \cdot \eta \cdot V_f}{(\rho_P - \rho_F) \cdot g}} \quad (1)$$

Where

$D_H$	: $\mu\text{m}$	; Liquid droplet or particle larger than $D_H$ will fall out.
$\eta$	: $\text{Pa}\cdot\text{s}$	; Dynamic viscosity.
$V_f$	: $\text{m/s}$	; Fluid velocity.
$\rho_P$	: $\text{kg/m}^3$	; Density particle and/or droplet.
$\rho_F$	: $\text{kg/m}^3$	; Density fluid.
$g$	: $\text{m/s}^2$	; Gravitational constant

By installing the probe at an angle the vertical velocity will decrease, consequently smaller particles will fall out as well. Additionally there is another advantage installing the probe at an angle, liquid water droplets will fall out as well.

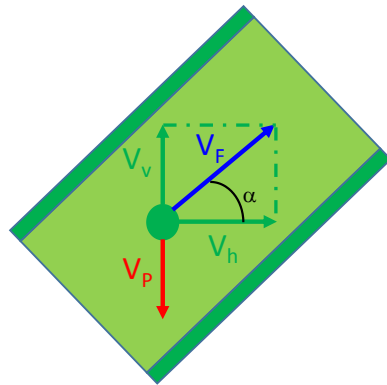


**FIGURE 9. INCLINED ORIENTATION.**

$$V_v = V_f * \text{SIN}\alpha \quad (2)$$

$$D_H = \sqrt{\frac{18*\eta*V_f*\text{SIN}\alpha}{(\rho_P-\rho_F)*g}} \quad (3)$$

$$V_h = V_f * \text{COS}\alpha \quad (4)$$

Where:

$V_f$	: $\text{m/s}$	; Fluid velocity.
$V_v$	: $\text{m/s}$	; Fluid velocity vertically.
$V_h$	: $\text{m/s}$	; Fluid velocity horizontally.
$\alpha$	: $^\circ$	; Angle probe

All liquid water droplets have the same horizontal velocity and will collide with the probe wall where they merge with the liquid film flowing back down the probe, into the process line.

## Experiments

A test was conducted on the flare gas probe by pulling a sample from the probe by means of a vacuum pump, creating a flow of approximately 90 NL/hr. Actual test conditions of flare gas upset conditions were simulated by means of a high pressure washer, simulating a high velocity and wet sample stream as shown on Figure 10.

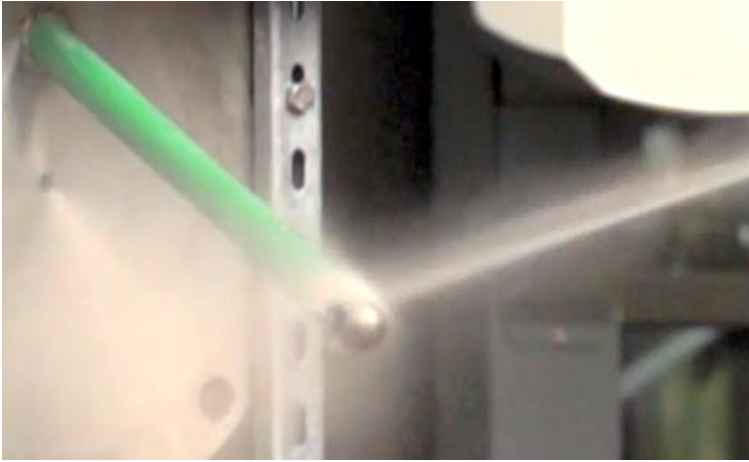


**FIGURE 10. HIGH VELOCITY AND WET PROCESS STREAM SIMULATION.**

In order to observe the behavior of the sample inside the probe a retractable camera was inserted into the probe via a gas tight gland seal. The position and view inside the probe are shown on Figure 11.

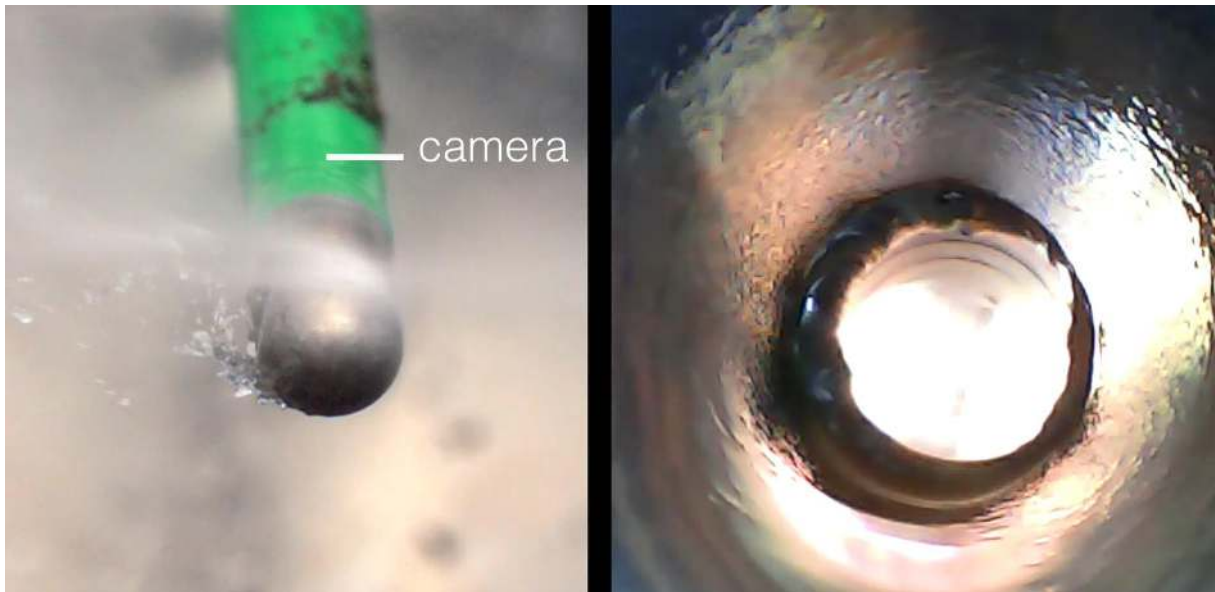


**FIGURE 11. DETAILS OF HIGH VELOCITY PROCESS STREAM AND VIEW FROM INSIDE THE FLARE GAS PROBE.**

In order to simulate high fouling at a high wet and high velocity process stream sand was manually added in large proportion to the high pressure washer jet as shown in Figure 12.



**FIGURE 12. HIGH VELOCITY AND WET PROCESS STREAM SIMULATION TOGETHER WITH SAND PARTICLES.**

With the retractable camera the probe inlet was observed during the test when excessive sand was added to the high pressure washer jet as shown in Figure 13. By the constantly changing light shade inside the probe it was observed that the excessive sand was passing by but not entering the probe.

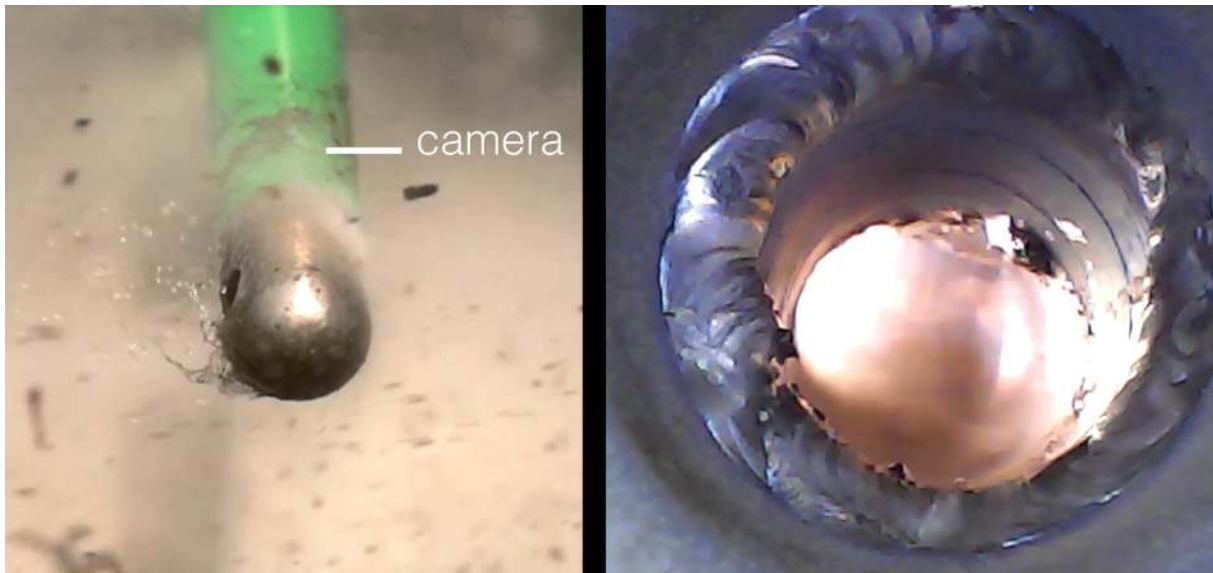


**FIGURE 13. DETAILS OF HIGH VELOCITY PROCESS STREAM WITH SEVERE PARTICLES AND VIEW FROM INSIDE THE FLARE GAS PROBE.**

### **Conclusions**

Customer feedback after start-up and operation was, Quote "Guys, back to office right now from inspection. Filters absolutely clean. Photos will follow in the next days. Seems everything works perfectly." Unquote.

The customer response to following question *This is really good news! Just a question did you have some upset conditions during the test!* response "Good question, I forgot to specify. Obviously I meant filters clean in presence of several upsets. We had 3 upsets and several small discharges since the installation." Unquote.

## **Acknowledgements**

The author like to thank Arno van Adrichem, Analyser Specialist and Discipline Technology Lead of ExxonMobil Research & Engineering and Salvatore Zocco, Measurement & Automation Technical Specialist of ESSO Italiana, Augusta Refinery for their trust, continuous support, and commitment to the development of the flare gas probe.

The author like to thank the ASaP engineering and R&D teams for their contribution and perseverance to make the development of the flare gas probe a success.

## **References**

1. Devenport. William, J. “-Experiment 3 – Flow past a circular cylinder”. Course manual AOE 3054 Experimental Methods. <http://www.dept.aoe.vt.edu/~devenpor/aoe3054/manual/expt3/>.
2. Gianoli, Doulgas, C., Physics for scientists and engineers, chapter 14, 25, 26, 19.
3. Pelević, Nikola, “ASAP IFBSL - Probe’s Behavior Under Real Test Conditions - CFD Analysis –“
4. Van den Akker, Harrie, and Mudde, Rob, “Fysische transport verschijnselen”.
5. Waters, Tony, Industrial Sampling Systems, pp. 166 - 171.